Plasmonics (2018) 13:1265–1269
DOI 10.1007/s11468-017-0628-8

Synthesis and Optical Properties of Highly Stabilized Peptide-Coated Silver Nanoparticles

P. Kalakonda[1,2] · **S. Banne**[3]

Received: 14 December 2016 / Accepted: 14 June 2017 / Published online: 26 June 2017

Abstract The interaction between peptide and silver nanoparticle surfaces has been increasingly of interest for bionanotechnology applications. To fully understand how to control such interactions, we have studied the optical properties of peptide-modified silver nanoparticles. However, the impacts of peptide binding motif upon the surface characteristics and physicochemical properties of nanoparticles remain not yet fully understood. Here, we have prepared sodium citrate-stabilized silver nanoparticles and coated with peptide IVD (ID_3). These nanomaterials were characterized by UV-visible, transmission electron microscopy (TEM), and z-potential measurement. The results indicate that silver nanoparticles (AgNP)-peptide interface is generated using ID_3 peptide and suggested that the reactivity of peptide is governed by the conformation of the bound peptide on the nanoparticle surface. The peptide-nanoparticle interactions could potentially be used to make specific functionality into the peptide capped nanomaterials and antibacterial applications.

Keywords Silver nanoparticles · Peptide · Z-potential · Physicochemical properties

✉ P. Kalakonda
parvathalu.k@gmail.com; pkalakon@cmu.edu

[1] Department of Materials Science and Engineering, Carnegie Mellon University, Pittsburgh, PA 15213, USA

[2] Department of Physics, Indian Institute of Science, Bangalore, KA, India

[3] School of Pharmaceutical Sciences and Innovative Drug Research Centre, Chongqing University, Chongqing, People's Republic of China

Introduction

In recent years, the synthesis of stable silver nanoparticles is one of the most leading active research in the field of nanotechnology because of their applications in broader areas such as bio-imaging, bio-medicine, bio-sensors, bio-labels, biomedical, antibacterial, catalysis, and diagnostics [1–9]. The metal nanoparticles must be capped appropriately to render them functional, biocompatible, and stable against aggregation in biological systems [10, 11] The main challenge is maintaining size and size distribution upon introduction into the biological environment. Ideally, the nanoparticle size should be between 10 and 100 nm to avoid renal clearance [12]and a neutral or negative charge to avoid phagocytic uptake. The adsorption of protein can drastically change the physicochemical properties of nanoparticles and affect their circulation, bio-distribution, and cellular internalization [13]. In addition, opsonization can result in undesired cellular uptake, nanoparticle aggregation, and an immune system response [14]..

The available methods for creating "stealth" nanoparticles that resist nonspecific protein adsorption include surface modification by polyethylene glycol (PEG) [15], polysaccharides [16], mixed charge self-assembly [17], and polymers [18, 19]. An attractive way for stealth coatings is to study the use of natural materials such as peptides: they are biocompatible, biodegradable, well-studied, non-immunogenic, and multifunctional materials [20]. Over the past few years, antibacterial peptides have become interesting tools in improving the new techniques for the production of novel antibiotics for the treatment of many human infections [21]. The antimicrobial activity of AgNP has been reported extensively in the killing of Gram-negative and Gram-positive bacteria [22, 23]. Silver nanoparticles are more toxic element to microorganism than any other metals; it slowly exhibits low toxicity to cells, and has a lower propensity to induce microbial resistance than any

other antimicrobial materials [24, 25]. Peptide-coated silver nanoparticles (PC-AgNP) have been studied to make stable systems in phosphate-buffered saline (PBS) [26, 27]. However, achieving stability in complex media such as undiluted human serum is even more challenging than in PBS due to the presence of thousands of proteins. The effect of interactions between PC-AgNPs and peptides were not yet fully studied. It is very important to study particles in complex media solutions before performing in vivo experiments. Developing PC-AgNPs that are stable in complex media can broaden in vivo applications and provide additional low fouling materials. In addition to possessing stealth properties, it is useful to incorporate specific interactions for biomedical technology applications. Many peptide sequences possess specific molecular recognition for receptors on various cell types. However, additional conjugation steps are needed to add peptide targeting sequences onto stealth particles containing synthetic low fouling polymers such as PEG [28, 29]. Peptide coatings offer an advantage because the targeting sequence can be extended off the existing peptide sequence [30, 31] avoiding complex conjugation steps. Combining the stealth peptide sequence with a targeting moiety achieves specific interactions while maintaining a low fouling background leading to increased stability in complex media and improved functionality.

In this work, we have designed a synthetic peptide of IVD (ID3) [32] associated with the amyloid disease. This indicates a strong hydration layer providing resistance to nonspecific protein adsorption. Furthermore, the sequence mimics the surfaces of proteins which have adapted to avoid nonspecific adsorption and display stability in complex media. Overall charge neutrality is maintained by leaving the N-terminus as a free amine, which contributes an extra positive charge to the peptide. The peptide sequence was attached to silver nanoparticles (AgNP) through the inclusion of a surface anchoring via covalent bonding to the silver surface. Optical spectroscopy (UV-visible) and zeta potential results indicate peptide capped silver nanoparticles display high stability. This multifunctional peptide contains biomolecular recognition, ultralow fouling, and surface anchoring in one sequence. Moreover, this system is easily constructed in one step process by mixing silver nanoparticles and self-assembling peptides.

Experimental Section

Materials and Methods

Silver nitrate ($AgNO_3$) and citric acid tri-sodium salt dehydrate were bought from Fisher Scientific (Waltham, MA). Peptide (ID3) with confirmed amino acid analysis (purity ≥95%) was purchased from the American Peptide Company. Net peptide content varied between 70 and 85%. The ID3 peptide was acetylated at the N-terminus. All solvents were purchased from Sigma-Aldrich Co. All these chemicals were analytical grade and used without any further purification.

Citrated Capped Silver Nanoparticles Synthesis Silver nanoparticles were synthesized by reduction of $AgNO_3$ with citric acid. The 90 mg of silver nitrate dissolved in 500 ml of aqueous solution was vigorously stirred and heated until it is steaming. To prepare ~30 nm diameter AgNPs, 10 ml solution of sodium citrate (1% by weight) was quickly added while steaming the AgNP solution. After the solution heated for another 10–15 min, the final solution was allowed to cool naturally to room temperature (Fig. 1).

Peptide-Coated AgNPs Peptide-coated AgNPs were prepared by mixing citrated capped AgNP with 0.5 mM peptide in aqueous solution. The solution was stirred for 10 min, and the self-assembled process was performed for 24 h.

Characterization of Silver Nanoparticles UV-visible absorption spectra were recorded at room temperature with a Smart Spec 3000 spectrophotometer from 300 to 800 nm. Fluorescence emission spectra were collected using a Horiba Fluoromax-4 spectrofluorometer. The chemical compositions of AgNPs solution were collected by using a Fourier transform infrared spectroscopy (ftir- 6700 Smart FTIR spectrometer ranging from 4000 to 400 cm-1. The silver nanoparticles size and morphology of particles were determined by TEM using a Tecnai G2 F20. Samples were prepared by evaporating 10 μl of AgNP solution onto carbon-supported copper grids. For the determination of particle size, over 300 particles were counted from multiple pictures from different areas of the TEM grid using image J software. The zeta potential of the particles was analyzed by using the Zeta-sizer Nano-ZS. Measurements were carried out at 25 °C in aqueous media. The zeta potential was calculated from the electrophoretic mobility based on the Smoluchowski theory.

Results and Discussion

The citrated-AgNPs and peptide-coated AgNPs were characterized by transmission electron microscopy (TEM) (Fig. 2). The diameter distribution of the AgNPs was measured using a TEM images analysis. The average diameter of the AgNPs, which were found to be 27 ± 3.0 nm (Fig. 2), was measured by

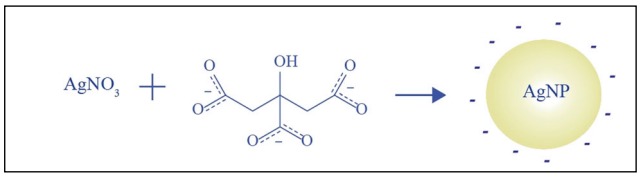

Fig. 1 Schematic of silver nanoparticles (AgNPs) synthesis

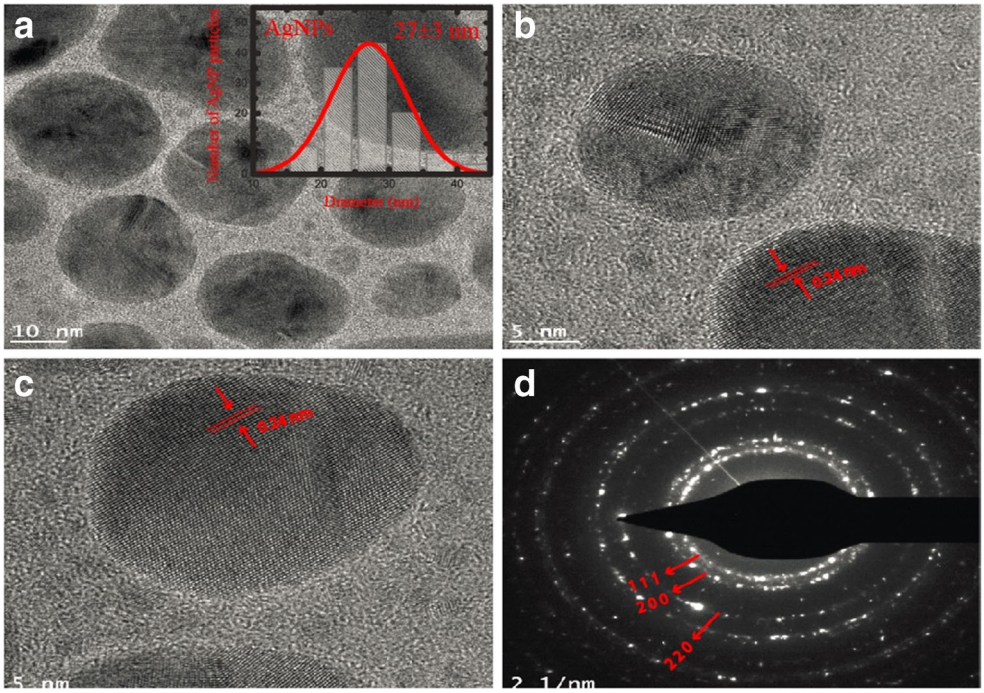

Fig. 2 The TEM images of AgNPs dispersion (**ac**) and a selected area of diffraction pattern of gold nanoparticles (**d**) and the insert show the diameter distribution of AgNPs (**a**)

statistical analysis of normal distribution. The TEM images of AgNPs were shown in Fig. 2a–c and peptide capped AgNP images were shown in Fig. 3a–b. Peptide capping does not affect the silver nanoparticle size if silver nanoparticles do not aggregate during the assembly process. On the basis of the HR-TEM images, and the constant silver core diameter, it is evident that PC-AgNPs remain monodispersed even after peptide capping (Fig. 3).

The HR-TEM image (Figs. 2 and 3) of AgNPs showed that the fringe spacing of AgNP was $2.4A^0$, which corresponded to the spacing between the plane of face-centered cubic (fcc) silver. The selected area of the diffraction pattern (SEAD) of silver nanoprism (Fig. 2d) indicated that the entire nanoparticle was monocrystalline structure [33]. The pattern of SEAD was indexed according to planes of (111), and (200) reflection of fcc silver on the basis of the d-spacing $2.4A^0$ and $2.04A^0$. The d-spacing were also calculated from diffraction pattern. The HR-TEM image of peptide-coated AgNPs showed (Fig. 3) that the thin layer of peptide coating was observed.

The FTIR spectra of citrate-stabilized AgNPs was performed to know about molecules present on the surface and showed the FTIR spectra (Fig. 4). FTIR spectrum shows absorption bands at 3350, 2914, 2855, 2354, 1740, 1632, 1455, 1377, 1242, and 1040 cm^{-1} and indicating the presence of capping agent with the AgNP. The bands at 3350 cm^{-1} in the spectra correspond to O-H stretching vibration indicating the presence of alcohol. Bands at 2914 and 2855 cm^{-1} region arising from C-H stretching of the aromatic groups were observed. The band at 1740 cm^{-1} was assigned for C-C band stretching. The band at 1632 cm^{-1} in the spectra corresponds to C-C and C-N stretching indicating the presence of proteins [34]. The band at 1455 cm^{-1} was assigned for N-H stretch vibration present in the amide linkages of the proteins. These functional groups have a role in stability and capping

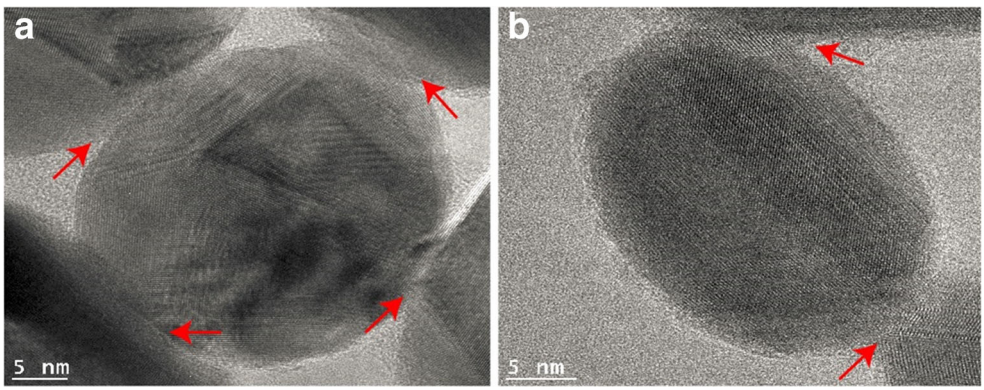

Fig. 3 HR-TEM image of peptide-coated AgNPs

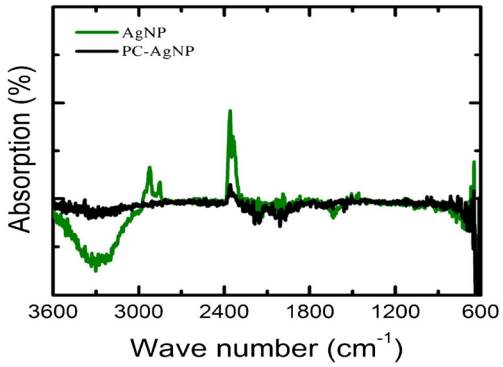

Fig. 4 FTIR spectra of silver nanoparticles

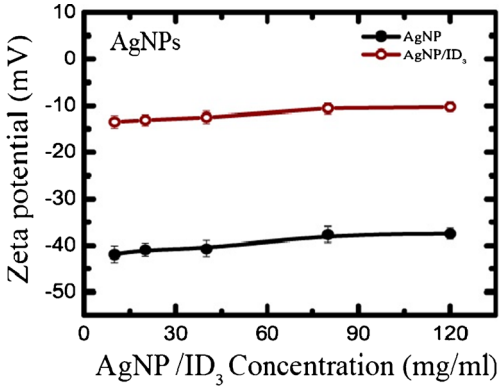

Fig. 6 **a** The zeta potential of AgNPs and AgNP/ID_3 as the function of concentration

of AgNP as reported in previous studies [34–37]. The bands at 1455 and 1040 cm^{-1} were assigned for N-H and C-N (amines) stretch vibration of the proteins, respectively. The band at 1377 cm^{-1} exemplifies the N-O symmetry stretching typical of the nitro compound. The PC-AgNP particles FTIR spectra were also collected and observed that the peaks were suppressed. It may be due to thin layer coating covered on the nanoparticles.

From UV-visible, citrated-AgNPs show a Plasmon band at 529 nm (Fig. 5a). The particle diameter can also be calculated from the concentration of silver nanoparticles and the absorbance at the surface Plasmon resonance and is in agreement with a diameter of 30 nm[36]. The surface Plasmon absorption spectrum of AgNP as the function of concentration is shown in Fig. 5a. The intensity of absorption spectra increased with increasing AgNP concentration. The trend was consistent with the changes corresponding to the surface Plasmon band of AgNPs. For peptide (ID_3)-coated AgNPs, the Plasmon band absorbance shifts to higher wavelength 404 nm Fig. 5b.

The hydrodynamic diameter of PC-AgNPs was measured by Zeta sizer to be 27 ± 3 nm. Zeta potential measurements indicate that the charge of the Cit-AgNP is −40 ± 2 mV (Fig. 6) in water and the charge of PC-AgNPs is −13 ± 1 mV. The differences observed between citrated-AgNPs and PC-AgNPs in UV-visible, TEM,and zeta potential measurements show evidence that the peptide is effectively capping the AgNPs. The shift to a higher Plasmon band and the hydrodynamic diameter size increase by about 1–2 nm after addition of peptide is consistent with the formation of a peptide layer on the surface of AgNPs [19]. Also, the reduction of charge from −40 to −13 mV (Fig. 6) indicates the displacement of negatively charged citric acid by the peptide. The slightly negative charge remaining on the PC-AgNPs is most likely due to a small amount of residual citrate molecules remaining on the surface after ligand exchange.

Stability in phosphate-buffered saline (PBS) is the first criteria for developing a robust, biocompatible system. However, if particles are to be utilized in more complex environments, such as in vivo, then harsher conditions need to be evaluated. Particle stability was assessed by monitoring the hydrodynamic diameter of particles using UV-visible, TEM,

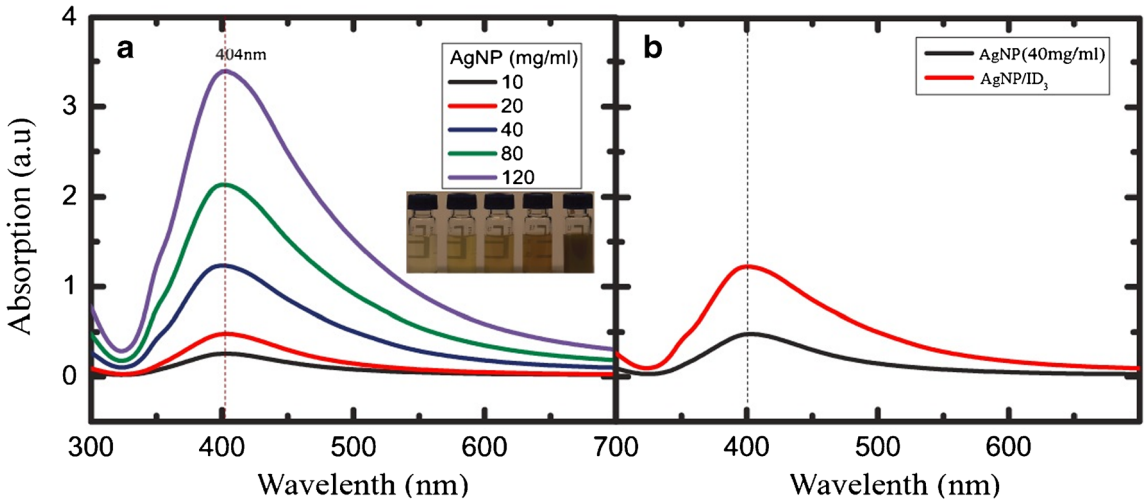

Fig. 5 **a** Absorption spectra peak intensity of AgNPs at different concentrations **b** Absorption spectra of AgNPs and AgNP/ID_3 at 30 mg/ml AgNPs concentration

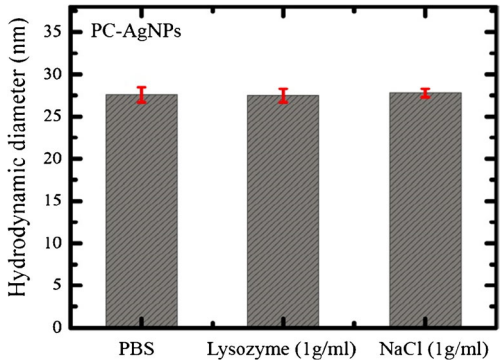

Fig. 7 DLS measurements of the hydrodynamic diameter (volume percentage) (nm) of PC-AgNPs after exposure to PBS, 1 mg/ml lysozyme in PBS, and 15 wt% NaCl solution for 50 min. Each data point represents an average value /standard deviation from three independent measurements

and DLS. As seen in Fig. 7, PC-AgNPs maintain the same hydrodynamic diameter (27 ± 3) after exposure to 15 wt% NaCl, 1 mg/ml lysozyme, and PBS solutions.

We examined PC-AgNP stability under high salt conditions. Most particles aggregate when the salt was added due to the screening of electrostatic repulsion; however, zwitterionic and mixed charge materials can resist aggregation due to the presence of a strongly bound surface hydration layer [18, 19]. In addition to examine particle stability in PBS solutions, the stability of PC-AgNPs was also measured at higher salt concentrations. PC-AgNPs maintain stability even at 15 (wt%) salt concentration. This result indicates the formation of a peptide-coated layer on the surface of silver nanoparticles.

Conclusion

In summary, the synthesis, characterization of silver nanoparticles capped with peptide material binding anchoring was demonstrated. These materials were generated through a simple reduction approach, which provides a general synthetic route that produced particles of similar size using peptides of binding affinity. The AgNPs were generally spherical with a relatively narrow size distribution. Peptide-coated AgNPs shows high stability in high salt concentration without any aggregating. The results suggest that the reactivity of the peptide on AgNPs surfaces is governed by the more details of the conformation of the bound peptide on the reconstructed nanoparticle surface as dictated by the peptide structure. These results may help for the use of peptides in the development of functional nanoparticles that exploit surface-based activity.

Acknowledgements Author would like to thank to WPI, USA, and IISc, Bangalore, India for financial support.

References

1. Baptista P, Pereira E, Eaton P, Doria G, Miranda A, Gomes I, Quaresma P, Franco R (2008) Anal Bioanal Chem 391(3):943–950
2. Dykman LA, Khlebtsov NG (2011) Acta Nat 3(2):34–55
3. Yeh YC, Creran B, Rotello VM (2012) Nano 4(6):1871–1880
4. Han M, Gao X, Su JZ, Nie S (2001) Nat Biotechnol 19(7):631–635
5. Huang X, El-Sayed IH, Qian W, El-Sayed MA (2006) J Am Chem Soc 128(6):2115–2120
6. Mirkin CA, Letsinger RL, Mucic RC, Storhoff JJ (1996) Nature 382(6592):607–609
7. Moreno-Manas M, Pleixats R (2003) Acc Chem Res 36(8):638–643
8. Salem AK, Searson PC, Leong KW (2003) Nat Mater 2(10):668–671
9. Kalakonda P, Banne S (2017) Nanotechnol Sci Appl 10:45–52
10. Peng ZA, Peng X (2002) J Am Chem Soc 124(13):3343–3353
11. Puntes VF, Krishnan KM, Alivisatos AP (2001) Science 291(5511): 2115–2117
12. Choi CHJ, Zuckerman JE, Webster P, Davis ME (2011) P Natl Acad Sci USA 108(16):6656–6661
13. Albanese A, Chan WC (2011) ACS Nano 5(7):5478–5489
14. Karmali PP, Simberg D (2011) Expert Opin Drug Del 8(3):343–357
15. Larson TA, Joshi PR, Sokolov K (2012) ACS Nano 6(10):9182–9190
16. Kodiyan A, Silva EA, Kim J, Aizenberg M, Mooney DJ (2012) ACS Nano 6(6):4796–4805
17. Liu XS, Chen YJ, Li H, Huang N, Jin Q, Ren KF, Ji J (2013) ACS Nano 7(7):6244–6257
18. Yang W, Zhang L, Wang SL, White AD, Jiang SY (2009) Biomaterials 30(29):5617–5621
19. Zhang L, Xue H, Gao CL, Carr L, Wang JN, Chu BC, Jiang SY (2010) Biomaterials 31(25):6582–6588
20. Collier JH, Segura T (2011) Biomaterials 32(18):4198–4204
21. Yoganathan V (2012) Evaluation of the effects of antimicrobial peptides on endodontic pathogens in vitro. Otago, Otago 131 p
22. Ansari MA, Khan HM, Khan AA (2011) Biol Med 3(2):141–146
23. Naqvi SZ, Kiran U, Ali MI, Jamal A, Hameed A, Ahmed S et al (2013) Int J Nanomedicine 8:3187–3195. doi:10.2147/IJN.S49284 [PubMed: 23986635]
24. Kora AJ, Arunachalam J (2011) World J Microbiol Biotech 27(5): 1209–1216. doi:10.1007/s11274-010-0569-2
25. Alizadeh H, Salouti M, Shapouri R. Jundishapur J Microbiol. 2014;**7**(3)
26. Levy R, Thanh NTK, Doty RC, Hussain I, Nichols RJ, Schiffrin DJ, Brust M, Fernig DG (2004) J Am Chem Soc 126(32):10076–10084
27. Olmedo I, Araya E, Sanz F, Medina E, Arbiol J, Toledo P, Alvarez-Lueje A, Giralt E, Kogan MJ (2008) Bioconjug Chem 19(6):1154–1163
28. Arosio D, Manzoni L, Araldi EM, Scolastico C (2011) Bioconjug Chem 22(4):664–672
29. Kim YH, Jeon J, Hong SH, Rhim WK, Lee YS, Youn H, Chung JK, Lee MC, Lee DS, Kang KW, Nam JM (2011) Small 7(14):2052–2060
30. Scari G, Porta F, Fascio U, Avvakumova S, Dal Santo V, De Simone M, Saviano M, Leone M, Del Gatto A, Pedone C, Zaccaro L (2012) Bioconjug Chem 23(3):340–349
31. Sun L, Liu D, Wang Z (2008) Langmuir 24(18):10293–10297
32. Reithofer MR, Lakshmanan A, Ping AT, Chin JM, Hauser CA (2014) Biomaterials 35(26):7535–7542
33. Khan MAM, Kumar S, Ahamed M, Alrokayan SA, AlSalhi M (2011) S 6(1):1–8
34. Prakash P, Gnanaprakasam P, Emmanuel R, Arokiyaraj S, Saravanan M (2013) Colloids Surf B: Biointerfaces 108:255–259(2013)
35. Chen S, Cao Z, Jiang S (2009) Biomaterials 30(29):5892–5896
36. Lin, K., Yi, J., Hu, S., Sun, J., Zheng, J., Wang, X., & Ren, B. 3 (7), 1248–1255, ACS Photonics(2016)
37. Mogensen KB, Katrin K (2014) J Phys Chem C 118(48):28075–28083